DESIGN OF ILC EXTRACTION LINE FOR 20 MRAD CROSSING ANGLE[*]

Y. Nosochkov[†], K. Moffeit, A. Seryi, M. Woods, SLAC, Menlo Park, CA 94025, USA
R. Arnold[‡], W. Oliver[§], B. Parker[¶], E. Torrence[‖]

Abstract

One of the two ILC Interaction Regions will have a large horizontal crossing angle which would allow to extract the spent beams in a separate beam line. In this paper, the extraction line design for 20 mrad crossing angle is presented. This beam line transports the primary e^+/e^- and beamstrahlung photon beams from the IP to a common dump, and includes diagnostic section for energy and polarization measurements. The optics is designed for a large energy acceptance to minimize losses in the low energy tail of the disrupted beam. The extraction optics, diagnostic instrumentation and particle tracking simulations are described.

INTRODUCTION

In a linear collider, the disruptive beam-beam forces at the Interaction Point (IP) do not affect beam dynamics upstream of the IP. Therefore, the beams can be focused to a very small size at the IP to attain high luminosity. However, the resultant high charge densities at the IP increase the non-linear beam-beam focusing which causes large particle deflections, emittance growth and radiation of beamstrahlung photons. As a result, two high power outgoing beams are created: the disrupted primary e^+/e^- with large angular divergence and low energy tail, and beamstrahlung photons. Since the total power in these beams will be as large as 10-20 MW, they have to be carefully transported to a dump with minimal losses. The collisions also generate secondary particles such as low energy e^+e^- pairs which add to power loss in the beginning of the extraction line.

Design of the International Linear Collider (ILC) calls for two Interaction Regions (IR) with a large and small crossing angle. The advantage of a small angle is that a crab cavity is not needed for collisions, but the small separation between the incoming and outgoing beams leads to a complicated extraction optics with shared quadrupoles. A large crossing angle allows an independent extraction line which is easier to design, but at the expense of a crab cavity.

Below, we present the extraction line design for a large 20 mrad horizontal crossing angle. In this design, the primary e^+/e^- and beamstrahlung photons travel through the same magnets to one shared dump, as in the NLC design[1]. The extraction optics also includes a diagnostic section for measurements of energy spectrum and polarization.

OPTICS

Lattice functions in the 20 mrad extraction line are shown in Fig.1, where the IP is at $s = 0$ and the dump is at ≈ 200 m. The optics consists of the DFDF quadruplet split in shorter quads, followed by two vertical chicanes for energy and polarization diagnostics, and a weak quadrupole doublet for mostly low energy focusing at the dump.

The first extraction quadrupole QDEX1 is placed at the same distance, 3.51 m after IP, as the first quad QD0 on incoming line. This choice is based on the SC compact quadrupole design[2] which makes it possible to have separate incoming and extraction SC quadrupoles despite a small 70 mm horizontal separation. The advantage of the side-by-side quad positions is that QDEX1 can also serve as a compensator for QD0 residual field on the extraction line. The QDEX1 gradient is chosen to be small, within 40 T/m, to reduce its fringe field on the incoming line to the IP. It is considered that quadrupoles up to $s = 11.5$ m will be superconducting, followed by warm magnets. The DFDF quadruplet includes a dedicated 2 m gap to provide space for the incoming crab-cavity.

The diagnostic section after the DFDF quadruplet includes two vertical chicanes for energy and polarization measurements with maximum vertical dispersion of 1.7 and 2 cm, respectively. The optics provides a 2nd focal point at the center of the polarimeter chicane to attain the required $< 100 \mu$m beam size. The D-polarity of the first quad after the IP makes it easier to attain the value of matrix term R_{22} at the 2nd focus close to -0.5 preferred for diagnostics, and improves focusing of low energy secondary particles vertically deflected in the detector solenoid[3].

The characteristic feature of the disrupted beam is a low energy tail which extends to $E/E_0 = 40 - 20\%$ for nominal ILC parameters and down to $< 10\%$ in high luminosity options[4]. Since deflections in magnets increase as E_0/E, the lowest energy particles are more likely to be lost. Due to significant beam power in the tail, a large chromatic acceptance is needed to minimize the beam loss. The
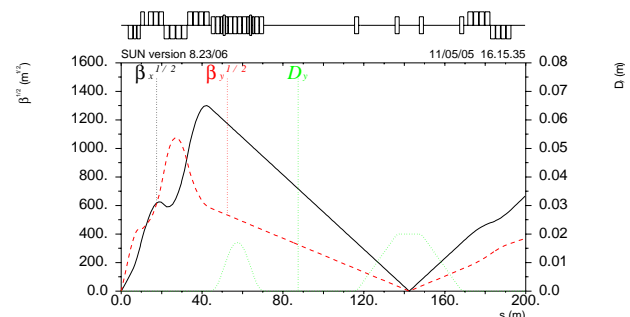

Figure 1: Lattice functions in the 20 mrad extraction line.

extraction acceptance was increased by using large apertures and optimizing chromatic focusing with the DFDF quadruplet. Compared to a simple doublet, the individual quadrupoles in the quadruplet are weaker, thus the low energy overfocusing is reduced. In addition, the apertures are chosen to accept the linearly divergent photon beam with conservatively large maximum IP angles of ± 1.25 mrad. The chicanes create orbit bumps which are closed for all energies. These bumps are included in bend apertures for $E/E_0 > 20\%$. Tracking showed that this optics accepts most particles with $E/E_0 > 40\%$ for the ILC parameters.

The detector solenoid field will create perturbations on the extraction optics. These effects were evaluated using a realistic 16.7 Tm solenoid field extending over 6.4 m after IP. Since the solenoid is at 10 mrad horizontal angle with respect to the beam, it would create a vertical orbit and dispersion on the order of several mm and cm, respectively, if not corrected. Additionally, the solenoid weak focusing would move the 2nd focus by $\Delta s \approx 1$ cm in the vertical plane. It was verified that the orbit can be canceled by $1-2$ kG correcting dipole windings on two SC quads which also reduce the residual dispersion to below a few mm. The solenoid focusing at the 2nd IP is easily corrected by a small adjustment of two quad gradients. After these corrections, the remaining solenoid perturbations have only minor effects on the extracted beam.

This extraction line is designed for up to 1 TeV center mass (CM) energy. The presently specified maximum field at magnet aperture is: 1.2 T in SC quads, 1 T in warm quads, and 0.834 T in the bends. The aperture varies from $r = 13$ to 28 mm in SC quads, from 41 to 83 mm in warm quads in the quadruplet, and is 250 mm in the doublet near the dump where the beam is large.

DIAGNOSTICS

The extraction line diagnostics will measure energy and polarization of the e^+/e^- beams. At present, the diagnostics are designed to accommodate a beam stayclear of an ± 0.75 mrad cone from the IP. A schematic for these diagnostics is shown in Fig.2.

The energy spectrometer measures the average beam energy by producing synchrotron radiation (SR) in wiggler magnets along the ± 2 mrad beam directions in the energy chicane. Two dipoles bend the beam up to the $+2$ mrad direction and the next four magnets bend the beam down to the -2 mrad direction. The distance between the SR stripes is about 40 cm at the detectors located at $s \approx 157$ m near the 2nd focus and is proportional to beam energy. The proportionality factor uses accurate measurements of $\int B ds$ and the distances between the magnets and the SR stripe detectors. A precision of 100 ppm is the design goal for the energy measurement[5].

The polarization measurement will be performed by a Compton polarimeter, with the Compton IP[6] (CIP) located at the 2nd focus. An accuracy of $\Delta P/P = 0.25\%$ should be achievable[5]. Vertical dispersion at the CIP is 2
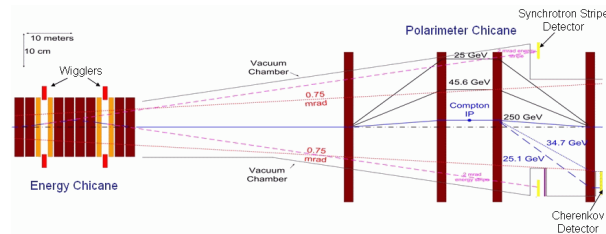

Figure 2: Diagram of the diagnostic section.

cm and there is no net bend angle with respect to the primary IP. Compton-scattered electrons near the kinematic edge at 25.1 GeV (for 250 GeV beam) are detected in a segmented detector located at $s \approx 170$ m. Beam-beam depolarization effects can be measured directly by comparing beams in and out of collision. Also, spin precession effects due to the final focus optics and beam-beam deflections can be studied by correlating the polarization and IP beam position monitor measurements. The matrix terms R_{22}, R_{44} give the angular magnification from the IP to the CIP. For polarimetry, R_{22} is most important since horizontal angles dominate. For $R_{22} = \pm 0.5$ the polarimeter measurement is close to the luminosity weighted polarization and is sensitive to both BMT and spin flip depolarization effects.

PARTICLE TRACKING

Simulation of beam transport from IP to dump was performed using the DIMAD code[7]. Beam distributions of up to $3.5 \cdot 10^7$ particles for the primary disrupted beam were generated in the GUINEA–PIG code[8] for the ILC "nominal" and "high luminosity" options of beam parameters at the IP[4]. Two cases were considered: 1) ideal collisions, and 2) collisions with large vertical beam-to-beam offset Δy. This offset may occur during initial IP tuning. It can increase the disrupted beam vertical divergence and result in higher beam loss[9]. Table 1 compares the maximum IP angles and the lowest relative energy E_{min}/E_0 in the disrupted beam for the nominal and high luminosity options at 0.5 TeV and 1 TeV CM energies. These parameters characterize the beam geometric and chromatic spread affecting the beam loss. The selected values of Δy correspond to about the largest disrupted IP angles.

One can see that at ideal collisions the disrupted beam size is larger in the horizontal plane, but the vertical size can dominate at a large Δy. The low energy tail increases with beam energy and is most significant in the high luminosity option. Summary of the total beam power loss is presented in Table 2. The results include the effect of detector solenoid with orbit and focusing correction assuming that IP orbit is canceled. At $\Delta y \neq 0$ (from Table 1), the beam loss is enhanced by the larger IP vertical angles. For comparison, the last row in Table 2 shows the beam power in the low energy tail with $E/E_0 < 40\%$. The tracking confirmed that most of the beam loss comes from this tail. For example, Fig.3 shows the relative energies of the lost particles versus the s-position of loss for 0.5 TeV CM high luminosity option. One can see that the extraction line

Table 1: Maximum IP angles and lowest relative energy in the disrupted beam for the ILC parameter options.

E_{CM} [TeV]	Δy [nm]	X'_{max} [μrad]	Y'_{max} [μrad]	E_{min}/E_0 [%]
0.5 nominal	0	529	253	36
	200	474	674	36
1.0 nominal	0	496	159	20
	100	423	566	19
0.5 high luminosity	0	1271	431	17
	120	1280	1415	17
1.0 high luminosity	0	2014	489	6.3
	80	1731	1592	6.2

Table 2: Total beam loss and power in tail with $\frac{E}{E_0} < 40\%$.

Parameter option		Nominal		High luminosity	
E_{CM} [TeV]		0.5	1.0	0.5	1.0
Total loss [kW]	$\Delta y = 0$	0	0.19	1.9	97
	$\Delta y \neq 0$	0.006	3.5	13.5	313
Tail power [kW]		0	1.3	3.9	146

accepts most particles with $E/E_0 > 40\%$, and the lowest energy particles are lost early in the beam line. Note that the vertical line pattern in Fig.3 is artificial because of the use of DIMAD output, where the loss is assigned to the end of elements.

Based on Table 2, the beam loss in the ILC nominal option appears acceptable. The high luminosity option may be acceptable at 0.5 TeV CM, but the beam loss is too high at 1 TeV CM. Following these results, there is a plan to optimize the 1 TeV CM high luminosity option in order to reduce the low energy tail. It is also important to attain a low density of power loss along the beam line, especially in the sensitive SC quads. Table 3 shows the maximum loss density in the SC quads and warm magnets, excluding the 1 TeV CM high luminosity option. The losses at $\Delta y = 0$ appear to be acceptable, but at large Δy the loss of up to ~ 600 W/m in warm magnets would need to be verified by the magnet design. Examples of the loss density in 0.5 TeV CM high luminosity and 1 TeV CM nominal option at $\Delta y = 0$ are shown in Fig.4,5.
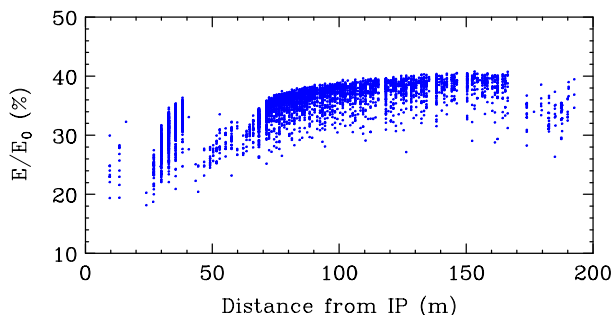

Figure 3: Relative energies of lost particles vs. s-position of loss for 0.5 TeV CM high luminosity option.

Table 3: Maximum density of power loss (W/m).

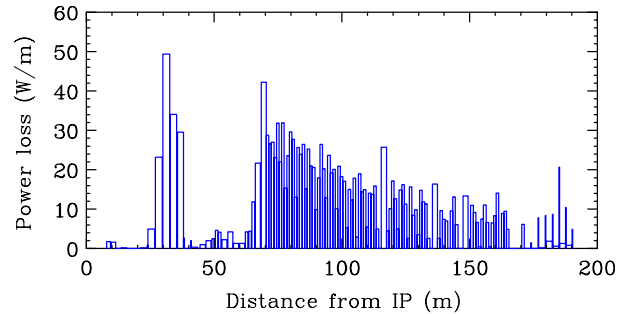| Parameter option		Nominal		High lumi
E_{CM} [TeV]		0.5	1.0	0.5
SC quads	$\Delta y = 0$	0	0	1.8
	$\Delta y \neq 0$	0	0	0
Warm magnets	$\Delta y = 0$	0	4.1	49
	$\Delta y \neq 0$	0.9	304	575

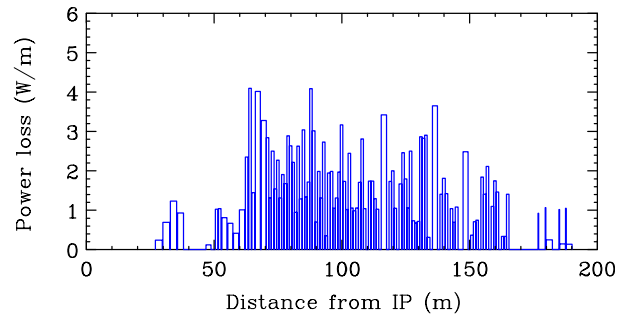Figure 4: Loss density for 0.5 TeV CM high luminosity.

Figure 5: Loss density for 1 TeV CM nominal case.

CONCLUSION

The presented 20 mrad extraction line provides the necessary optics for downstream diagnostics and sufficient beam acceptance for the ILC nominal parameters up to 1 TeV CM. It may be also suitable for the 0.5 TeV CM high luminosity option. Further studies will include a detailed magnet design, optimization of beam spot at the dump and a possibility of collimation to reduce the maximum density of beam loss.

REFERENCES

[1] Y. Nosochkov, et al., SLAC–PUB–8096 (1999).
[2] B. Parker, et al., "Compact Superconducting Final Focus Magnet Options for the ILC," these proceedings.
[3] T. Maruyama, private communication.
[4] T. Raubenheimer, http://www-project.slac.stanford.edu/ilc/acceldev/beamparameters.html (February 28, 2005).
[5] D. Cinabro, et al., IPBI TN–2003–1 (2003).
[6] K.C. Moffeit, M. Woods, IPBI TN–2003–2 (2003).
[7] http://www.slac.stanford.edu/accel/ilc/codes/dimad/ .
[8] D. Schulte, "Beam-Beam Simulations with GUINEA–PIG," ICAP98, Monterey, CA, USA (1998).
[9] Y. Nosochkov, et al., SLAC–PUB–8872 (2001).